Available online at www.sciencedirect.com
ScienceDirect
Trans. Nonferrous Met. Soc. China 27(2017) 1081−1086
Transactions of Nonferrous Metals Society of China
www.tnmsc.cn

In vitro corrosion resistance and antibacterial properties of layer-by-layer assembled chitosan/poly-L-glutamic acid coating on AZ31 magnesium alloys

Lan-yue CUI[1,2], Ji XU[1], Na LU[1], Rong-chang ZENG[1,2], Yu-hong ZOU[3], Shuo-qi LI[1,2], Fen ZHANG[1,2]

1. College of Materials Science and Engineering,
Shandong University of Science and Technology, Qingdao 266590, China;
2. State Key Laboratory of Mining Disaster Prevention and Control Co-founded by Shandong Province and the Ministry of Science and Technology, Shandong University of Science and Technology, Qingdao 266590, China;
3. College of Chemical and Environmental Engineering,
Shandong University of Science and Technology, Qingdao 266590, China

Received 22 May 2016; accepted 16 December 2016

Abstract: Surface functionalization of magnesium (Mg) alloys is desired to obtain the surfaces with both improved corrosion resistance and antibacterial property. A corrosion-resistant and antimicrobial coating was prepared on Mg alloy surface by layer-by-layer (LbL) assembly of chitosan (CHI) and poly-L-glutamic acid (PGA) by electrostatic attraction. The functionalized surfaces of the Mg alloys were characterized by field-emission scanning electron microscopy (FE-SEM), Fourier transform infrared (FT-IR) spectroscopy and electrochemical tests. The bactericidal activity of the samples against *Staphylococcus aureus* was assessed by the zone of plate-counting method. The obtained coating on the Mg alloy substrates exhibits good corrosion resistance and antibacterial performance.

Key words: magnesium alloy; corrosion; layer-by-layer assembly; chitosan; antibacterial effect

1 Introduction

Magnesium (Mg) and its alloys hold promise in the biomedical metal materials owing to their unique biodegradability, good biocompatibility and bio-mechanical compatibility [1−5]. However, the potential clinical applications of Mg alloys are hindered by their poor corrosion resistance in the human body [6−10]. And the antibacterial performance is also desired for the biomedical applications of the Mg alloys [11].

Surface modification on Mg alloys is highly desirable to improve their biocompatibility by reducing the corrosion rate and enhancing the antimicrobial properties [12]. Among all the surface modification methods, the layer-by-layer (LbL) self-assembly technique is a versatile and simple method for the incorporation of polyelectrolytes into biomedical coatings by the principle of electrostatic attractive forces between the oppositely charged building blocks [13−16]. Previously, we constructed a (poly(sodium 4-styrene sulfonate)/gentamicin sulfate)$_n$ coating [17] and a polysiloxane/(poly(acrylic acid)/gentamicin sulfate)$_{20}$/Mg composite coating [18] via LbL self-assembly to enhance the corrosion resistance and antimicrobial function. However, it is the main limitation that more and more kinds of bacteria show resistance and side-effects to antibiotics on mammal cells or tissues [19].

The polyelectrolytes, e.g., poly-L-glutamic acid (PGA) and chitosan (CHI), are both useful biological materials [20]. PGA, a synthetic polypeptide (solution pK_a=4.4 [21]), is a promising material in tissue engineering because of its good hydrophilicity, biodegradability and non-toxic features [22]. CHI (pK_a=6.5 [23]) is a cationic natural polymer that carries positive charges with a molecular structure of (1 and 4)-linked 2-amino-2-deoxy-β-d-glucan [24]. CHI is also reported to exhibit inherent antimicrobial properties and

Foundation item: Projects (51571134, 51601108) supported by the National Natural Science Foundation of China; Project (2013RCJJ006) supported by the Scientific Research Foundation of Shandong University of Science and Technology for Recruited Talents, China; Project (2016ZRB01A62) supported by the Natural Science Foundation of Shandong Province, China; Project (2014TDJH104) supported by Shandong University of Science and Technology Research Fund, China
Corresponding author: Rong-chang ZENG; Tel: +86-532-86051385; E-mail: rczeng@foxmail.com
DOI: 10.1016/S1003-6326(17)60126-2

antibiofilm behaviors [19], which leads to the wide usage in drug formulations [25], tissue engineering [26] and antibacterial treatments [25].

The purpose of this work is to assess the feasibility of constructing antibacterial multilayer films with CHI as polycation and PGA as polyanion on Mg alloy AZ31. CHI can be positively charged when the solution pH is lower than its pK_a and PGA can be negitively charged when the solution pH is higher than its pK_a. Thus, the polyelectrolyte-multilyers (PEMs) can be fabricated through the electrostatic forces between CHI and PGA. The corrosion resistance and antimicrobial properties of the PEMs are investigated. The biocompatible CHI and PGA are chosen due to the fact that they offer the opportunities to design new antimicrobial materials without using the antibiotics.

2 Experimental

AZ31 alloy (composition in mass fraction, %: Al 2.5−3.0, Zn 0.7−1.3, Mn >0.20, Si ≤0.3, Cu ≤0.05, Ni ≤0.005, Fe ≤0.005 and balanced Mg, size: 20 mm × 20 mm × 3 mm) specimens were ground with sand papers up to 1500 grit followed by wash with deionized (DI) water and alcohol solution and dried by warm air. The treated substrates were then soaked in a 1 mol/L NaOH solution for 20 min to obtaine hydroxylate surface with stirring, followed by thorough cleaning with DI water and drying with warm air. The prepared samples were denoted as NaOH-treated AZ31.

The PEMs were prepared using a dip-coating method. Layers were generated in the following sequence: "ABCBCBCBCBC". Solutions A and B contained the cationic polyethyleneimine (PEI) (5 g/L, pH 9.0, relative molecular mass 600, 99.0%) and the anionic PGA (3 g/L, pH 6.2). And solutions C contained the cationic CHI (3 g/L, pH 5.0, 99%) and acetic acid (1%, volume fraction). The substrate was dipped into solution A for 30 min, and solution B and solution C for 5 min. Five cycles were performed during the deposition experiment to obtain $(CHI/PGA)_5$/AZ31 samples. The preparation process and the chemical structures of the PEI, PGA, and CHI were schematically illustrated in Fig. 1.

The surface morphologies of the films were studied using field-emission scanning electron microscopy (FE-SEM, Nova NanoSEM 450, USA). The possible chemical bondings formed in the coatings were confirmed using a Fourier transform infrared (FTIR) spectrophotometer (Nicolet380, Thermo Electron Corporation, USA), and the coating was detached from the alloy surface before the test.

The potentiodynamic polarization curves and electrochemical impedance spectra (EIS) were obtained using an electrochemical analyser (PAR Model 2273, Princeton, USA). A three-electrode cell set-up was used, in which the prepared samples were the working electrode and a saturated calomel electrode and a platinum sheet were used as the reference and counter electrodes, respectively. The polarization started from approximately −2000 to −1000 mV at a scan rate of 1 mV/s. EIS studies were performed at open-circuit potential for a 10 mV sinusoidal amplitude over a frequency range of 100 kHz to 0.01 Hz. A stable open-circuit potential about 600 s was established prior to testing. The experiment was conducted in a simulated body fluid (SBF) solution (8.035 g/L NaCl, 0.225 g/L KCl, 0.292 g/L $CaCl_2$, 0.335 g/L $NaHCO_3$, 0.423 g/L $MgCl_2·6H_2O$, 0.272 g/L Na_2SO_4, 0.231 g/L $KH_2PO_4·3H_2O$, and 6.228 g/L Tris·HCl buffer).

The antibacterial effects of the samples were evaluated by plane-counting method. Gram-positive *Staphylococcus aureus (S. aureus)* were cultured in agar plates at 37 °C overnight. The agar plates (pH 7.2−7.4) were composed of 5 g/L beef extract powder, 10 g/L tryptone, 5 g/L NaCl and 20 g/L agar. Then, the AZ31, $(CHI/PGA)_5$/AZ31 samples were placed on the inoculated agar plates and incubated at 37 °C for 24 h. Bacterial colonies can be easily captured and countable.

3 Results and discussion

3.1 Surface morphology

Figure 2 shows the SEM morphologies of the NaOH-treated AZ31 and $(CHI/PGA)_5$/AZ31 coatings. The pristine Mg alloy displays visible scratches

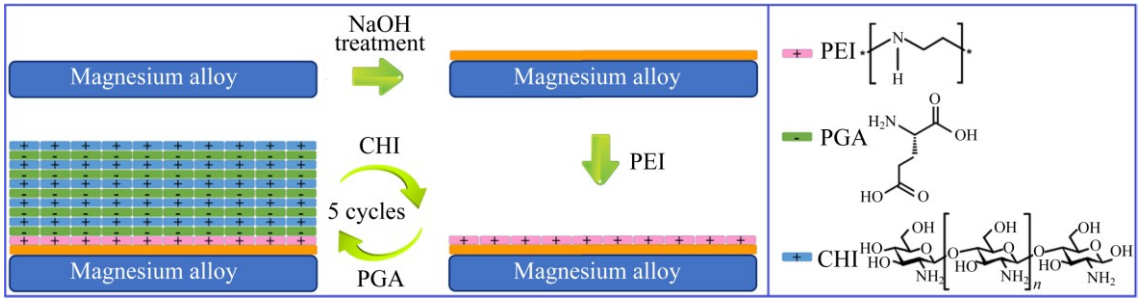

Fig. 1 Preparation process and chemical structures of PEI, PGA, and CHI

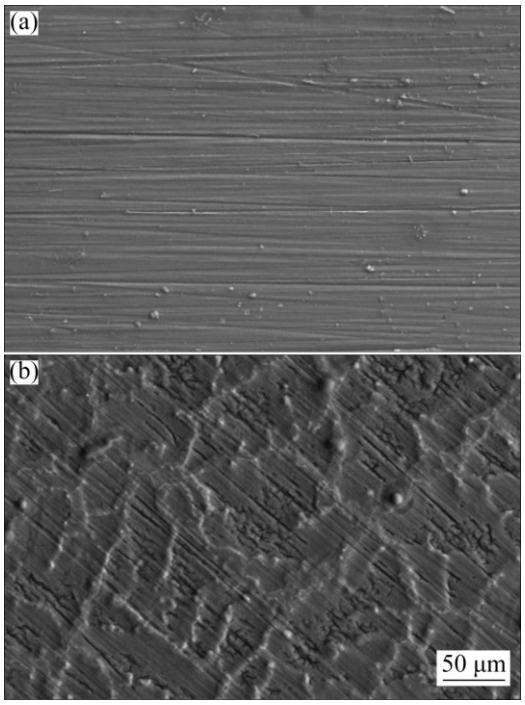

Fig. 2 SEM morphologies of NaOH-treated AZ31 (a) and $(CHI/PGA)_5$/AZ31 coatings (b)

(Fig. 2(a)), which are attributed to the grinding process. While for the $(CHI/PGA)_5$/AZ31 coating (Fig. 2(b)), the rough surface with deepening scratches implies the combination of dissolution of Mg and deposition of a thinner film.

FT-IR was utilized to analyze the chemical composition of the $(CHI/PGA)_5$/AZ31 surface (Fig. 3). For a comparison, the FT-IR spectra of pure PGA and CHI were also measured. And the spectra of the CHI/PGA multilayers feature similar characteristic peaks to those of their parent polymers. For the spectra of the $(CHI/PGA)_5$, the characteristic saccharide peaks of CHI in the 960−1180 cm^{-1} region were observed: the C—O stretching absorption band at 1097 and 1032 cm^{-1} and the C—O—C asymmetric stretching vibrations at ~1154 cm^{-1} [27]. On the other hand, the peaks of amide I and II groups of PGA are located at 1637 and 1590 cm^{-1}, respectively. And in the assembled films, higher frequency shifts of amide I, amide II and C—O are found, ascribed to the strong electrostatic interaction between the —COOH of PGA and the $—NH_2$ of CHI [28]. Thus, the results of FTIR analysis clearly prove the successful fabrication of the $(CHI/PGA)_5$ multilayers.

3.2 Corrosion resistance

Figure 4(a) shows the polarization curves using Tafel extrapolation. The corrosion potential (φ_{corr}) shifts to a more negative value from −1.47 V (vs SCE) of the substrate to −1.67 V (vs SCE) of the multilayer surface, which is ascribed to the formation of the hydroxide film

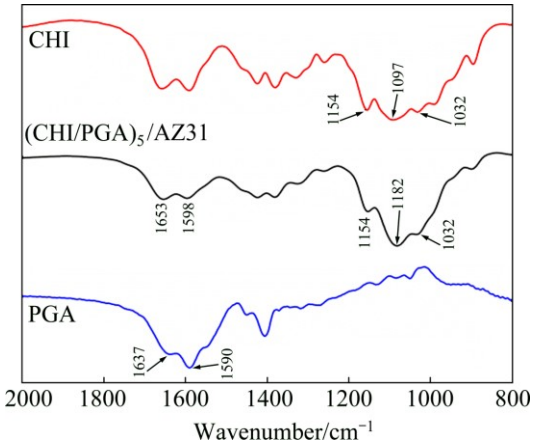

Fig. 3 FT-IR spectra of pure CHI, $(CHI/PGA)_5$/AZ31 coating and pure PGA

after immersion of the alloy samples in the NaOH solution. Accordingly, the corrosion current density (J_{corr}) of the $(CHI/PGA)_5$/AZ31 coating surfaces is 4.04×10^{-7} A/cm^2, which decreases by more than one order of magnitude compared to that of the substrate (6.85×10^{-6} A/cm^2). The decreased J_{corr} reveals that the $(CHI/PGA)_5$/ AZ31 coating improves the corrosion resistance of AZ31 alloy. Figure 4(b) shows the Nyquist plots for the EIS studies. Two capacitive loops were observed for the plots of both the substrate and $(CHI/PGA)_5$/AZ31 sample. It is well known that the capacitive loop in the high frequency range can be attributed to the charge transfer reaction and the diameter of the loop is proportional to the value of the transfer resistance. The larger value the transfer resistance has, the better the corrosion resistance is. The diameter (8.32 kΩ) of the loop for the $(CHI/PGA)_5$/AZ31 is more than 20 times larger than that (0.38 kΩ) of the substrate, indicating an increase in corrosion resistance of the $(CHI/PGA)_5$/AZ31 coating. Moreover, the low-frequency impedance modulus $|Z|$ is one of the parameters used to evaluate the corrosion resistance of different samples in Bode plots [29,30] (Fig. 4(c)). A larger $|Z|$ indicates a better corrosion protection performance. It can be observed that the $|Z|$ increases with surface modification on the AZ31 substrate, indicating the beneficial effect of the multilayer in improving the corrosion resistance of the Mg alloy. The results are in agreement with the polarization curves.

These experimental data can be accurately fitted to the equivalent circuit $R_s(Q_1(R_{c1}(CR_{ct})))$ and $R_s(Q_1(R_{c1}(Q_2(R_{c2}(CR_{ct})))))$ (Figs. 4(d) and (e)) [3,15]. In these models, R_s represents the solution resistance between the reference and working electrodes, R_{ct} is the charge transfer resistance relating to the electrochemical reaction, and R_c is the coating resistance paralleled with a constant phase element (CPE). Based on the proposed

equivalent circuit models and the properties of the coating, EIS curves are best fitted, and the corresponding values of the equivalent circuit parameters are listed in Table 1. Generally, a higher R_{ct} value implies a lower dissolution rate. The lower R_{ct} of the Mg substrate (approximately 0.36 kΩ) suggests a high corrosion rate. The increased value of R_{ct} (approximately 24.27 kΩ) for the LbL-assembled films emphasizes the beneficial effect of the $(CHI/PGA)_5$/AZ31 coating.

The improvement in the corrosion resistance may be ascribed to the fact that weak-weak polyelectrolytes pair can provide pH buffering action due to their ability to dissociate in either acidic or basic conditions [31]. Extraordinarily, it is demonstrated that the CHI possesses the function as a reservoir for active species for corrosion protection [32]. The capacity of CHI to form good films and the reversibility of charging CHI amine groups provide foundations for further development of active/'smart' coatings, and extend the application of this polymer to other active metal substrates.

3.3 Antibacterial effect

The antibacterial effect of the substrate and $(CHI/PGA)_5$/AZ31, evaluated by the plate-counting method is shown in Fig. 5. Compared with the bare AZ31 alloy (411±17 CFU), the $(CHI/PGA)_5$/AZ31 (11±2 CPU) shows better antibacterial activity due to the fact that the PGA/CHI inhibits the growth of *S. aureus*. The scenario may be ascribed to the contact-killing strategy. The coating surfaces are capable of killing bacteria through a direct contact [19,33]. Thus, the PEMs, targeting bacterial membranes, are promising routes for preventing immune rejection of implanted Mg alloys, as they are less likely to lead to bacterial resistance compared to protein-targeting antibacterial agents such as antibiotics [34,35].

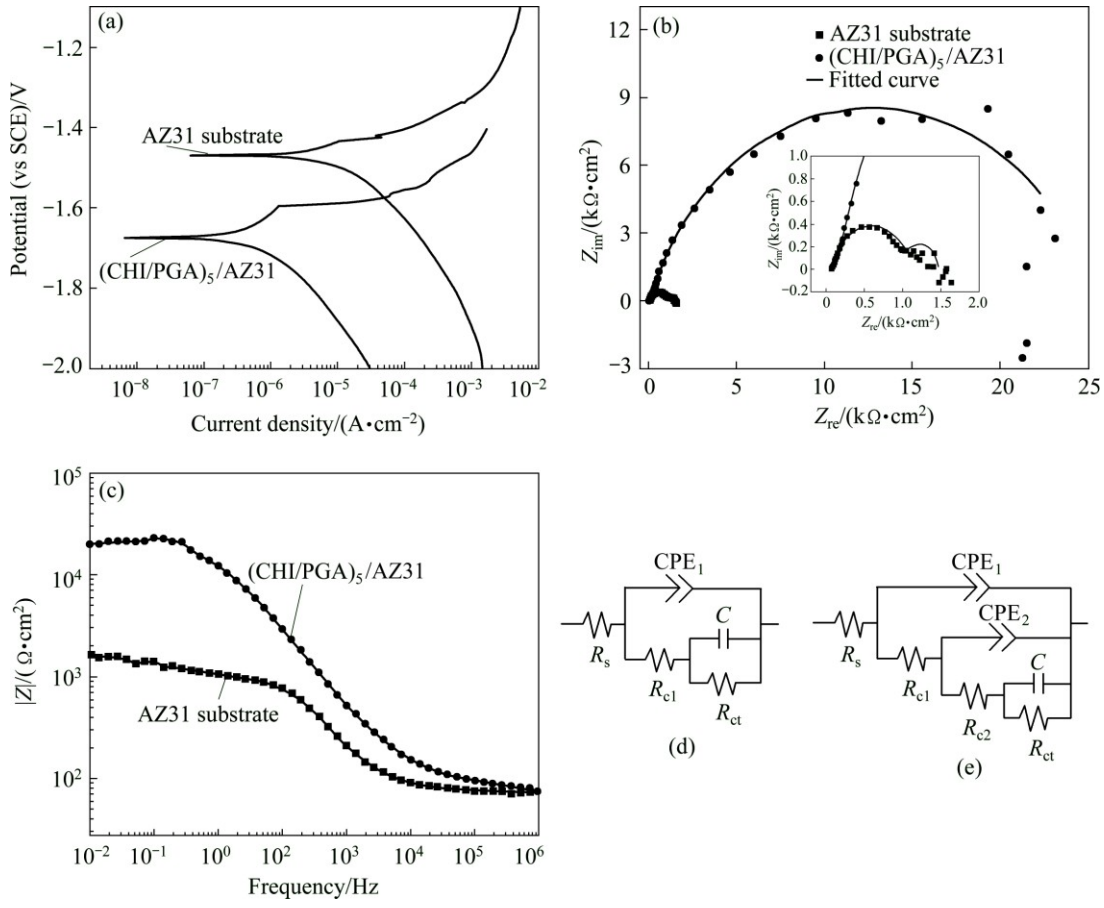

Fig. 4 Electrochemical measurements of substrate and $(CHI/PGA)_5$/AZ31 surfaces: (a) Polarization curves; (b) Nyquist plots; (c) Bode plots; (d, e) Equivalent circuits

Table 1 Parameter values of electrical circuits of samples

Sample	R_s/ ($\Omega\cdot cm^2$)	Q_1/ ($\Omega^{-1}\cdot s^n\cdot cm^{-2}$)	n_1	R_{c1}/ ($\Omega\cdot cm^2$)	Q_2/ ($\Omega^{-1}\cdot s^n\cdot cm^{-2}$)	n_2	R_{c2}/ ($\Omega\cdot cm^2$)	C/ ($F\cdot cm^{-2}$)	R_{ct}/ ($\Omega\cdot cm^2$)
Substrate	75.57	2.79×10^{-5}	0.82	1028	–	–	–	2.19×10^{-3}	359.30
$(CHI/PGA)_5$/AZ31	79.03	1.30×10^{-5}	0.72	135.5	7.96×10^{-7}	0.97	1249	5.88×10^{-7}	2.43×10^{4}

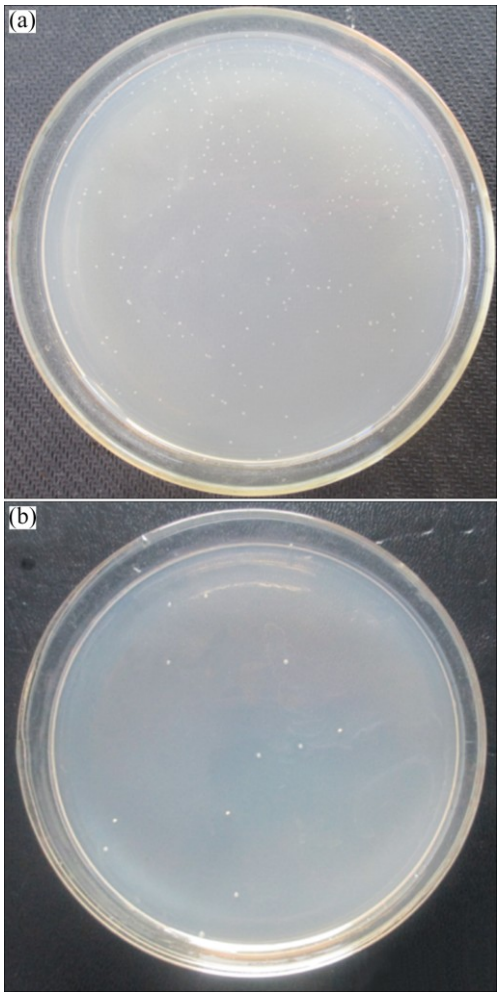

Fig. 5 Comparison of antibacterial effect of substrate (a) and $(CHI/PGA)_5$/AZ31 sample (b) evaluated by plate-counting method

4 Conclusions

1) The positively charged CHI and the negatively charged PGA were successfully alternatively immobilized onto the surface of Mg alloys via LbL self-assembly technique.

2) The morphologies of LbL films coated Mg alloys were greatly influenced by the polyelectrolyte immersion process. Compared with the bare AZ31 alloy, the obtained surface showed a good corrosion resistance when immersed in SBF solution, due to the pH buffering action of the weak-weak polyelectrolytes pair.

3) The good antibacterial property was obtained, which can be ascribed to the contact-killing strategy.

References

[1] ZHENG Yu-feng, GU Xue-nan, WITTE F. Biodegradable metals [J]. Materials Science & Engineering R, 2014, 77: 1−34.

[2] HENDERSON S E, VERDELIS K, MAITI S, PAL S, CHUNG W L, CHOU D T, KUNTA P N, ALMARZA A J. Magnesium alloys as a biomaterial for degradable craniofacial screws [J]. Acta Biomaterialia, 2014, 10: 2323−2332.

[3] ZENG Rong-chang, CUI Lan-yue, JIANG Ke, LIU Rui, ZHAO Bao-dong, ZHENG Yu-feng. In vitro corrosion and cytocompatibility of a microarc oxidation coating and poly(L-lactic acid) composite coating on Mg−1Li−1Ca alloy for orthopedic implants [J]. ACS Applied Materials & Interfaces, 2016, 8: 10014−10028.

[4] ZENG Rong-chang, QI Wei-chen, SONG Ying-wei, HE Qing-kun, CUI Hong-zhi, HAN En-hou. In vitro degradation of MAO/PLA coating on Mg−1.21Li−1.12Ca−1.0Y alloy [J]. Frontiers of Materials Science, 2014, 8: 343−353.

[5] ZENG Rong-chang, LI Xiao-ting, LI Shuo-qi, ZHANG Fen, HAN En-hou. In vitro degradation of pure Mg in response to glucose [J]. Scientific Reports, 2015, 5: 13026. Doi: 10.1038/srep13026.

[6] ZENG Rong-chang, LI Xiao-ting, LIU Li-jun, LI Shuo-qi, ZHANG Fen. In vitro degradation of pure Mg for esophageal stent in artificial saliva [J]. Journal of Materials Science & Technology, 2016, 32: 437−444.

[7] ZENG Rong-chang, ZHANG Fen, LAN Zi-dong, CUI Hong-zhi, HAN En-hou. Corrosion resistance of calcium-modified zinc phosphate conversion coatings on magnesium-aluminium alloys [J]. Corrosion Science, 2014, 88: 452−459.

[8] ZENG Rong-chang, HU Yan, ZHANG Fen, HUANG Yuan-ding, WANG Zhen-lin, LI Shuo-qi, HAN En-hou. Corrosion resistance of cerium-doped zinc calcium phosphate chemical conversion coatings on AZ31 magnesium alloy [J]. Transactions of Nonferrous Metals Society of China, 2016, 26: 472−483.

[9] CHENG Ying-liang, WU Hai-lan, CHEN Zhen-hua, WANG Hui-min, ZHANG Zhao, WU You-wu. Corrosion properties of AZ31 magnesium alloy and protective effects of chemical conversion layers and anodized-coatings [J]. Transactions of Nonferrous Metals Society of China, 2007, 17: 502−508.

[10] LIU Fen-jun, MENG Qing-sen, LI Zeng-sheng. Microstructure and properties of alloying coating on AZ31B magnesium alloy [J]. Transactions of Nonferrous Metals Society of China, 2016, 26: 2347−2354.

[11] KURISSERY S R, KANAVILLIL N, KIKUCHI Y. Bacterial attachment on magnesium alloy AZ31B with a note on its antibacterial property (materials, metallurgy & weldability) [J]. Transactions of JWRI, 2002, 31: 55−61.

[12] LU Ping, LIU Yin, GUO Mei-qing, FANG Hai-dong, XU Xin-hua. Corrosion and drug release properties of EN-plating/PLGA composite coating on MAO film [J]. Materials Science & Engineering C, 2011, 31: 1285−1289.

[13] ZHANG Xiao-dan, YI Jin-hong, ZHAO Guo-wei, HUANG Lin-lin, YAN Guang-jun, CHEN Ya-shao, LIU Peng. Layer-by-layer assembly of silver nanoparticles embedded polyelectrolyte multilayer on magnesium alloy with enhanced antibacterial property [J]. Surface & Coatings Technology, 2016, 286: 103−112.

[14] LI Hui, PENG Lin-cai. Antimicrobial and antioxidant surface modification of cellulose fibers using layer-by-layer deposition of chitosan and lignosulfonates [J]. Carbohydrate Polymers, 2015, 124: 35−42.

[15] CUI Lan-yue, ZENG Rong-chang, LI Shuo-qi, ZHANG Fen, HAN En-hou. Corrosion resistance of layer-by-layer assembled polyvinylpyrrolidone/polyacrylic acid and amorphous silica films on AZ31 magnesium alloys [J]. RSC Advances, 2016, 6: 63107−63116.

[16] CUI Lan-yue, ZENG Rong-chang, ZHU Xiao-xiao, PANG Ting-ting, LI Shuo-qi, ZHANG Fen. Corrosion resistance of biodegradable polymeric layer-by-layer coatings on magnesium alloy AZ31 [J]. Frontiers of Materials Science, 2016, 10: 134−146.

[17] ZENG Rong-chang, LIU Li-jun, LUO Kai-jie, SHEN Li, ZHANG Fen, LI Shuo-qi, ZOU Yu-hong. In vitro corrosion and antibacterial properties of layer-by-layer assembled GS/PSS coating on AZ31

magnesium alloys [J]. Transactions of Nonferrous Metals Society of China, 2015, 25: 4028−4039.

[18] LIU Li-jun, LI Ping-ping, ZOU Yu-hong, LUO Kai-jie, ZHANG Fen, ZENG Rong-chang, LI Shuo-qi. In vitro corrosion and antibacterial performance of polysiloxane and poly(acrylic acid)/gentamicin sulfate composite coatings on AZ31 alloy [J]. Surface & Coatings Technology, 2016, 291: 7−14.

[19] WANG Bai-liang, REN Ke-fang, CHANG Hao, WANG Jin-lei, JI Jian. Construction of degradable multilayer films for enhanced antibacterial properties [J]. ACS Applied Materials & Interfaces, 2013, 5: 4136−4143.

[20] SONG Zhi-jiang, YIN Jing-bo, LUO Kun, ZHENG Yan-zhen, YANG Yan, LI Qiong, YAN Ahi-feng, CHEN Xue-si. Layer-by-layer buildup of poly(L-glutamic acid)/chitosan film for biologically active coating [J]. Macromolecular Bioscience, 2009, 9: 268−278.

[21] LI Chun. Poly(L-glutamic acid)-anticancer drug conjugates [J]. Advanced Drug Delivery Reviews, 2002, 54: 695−713.

[22] ZHAO N, YANG C, WANG Y, ZHAO B, BIAN F, LI X, WANG J. Probing the surface microstructure of layer-by-layer self-assembly chitosan/poly(l-glutamic acid) multilayers: A grazing-incidence small-angle X-ray scattering study [J]. Materials Science & Engineering C, 2016, 58: 352−358.

[23] OTANI Y, TABATA Y, IKADA Y. Rapidly curable biological glue composed of gelatin and poly(L-glutamic acid) [J]. Biomaterials, 1996, 17: 1387−1391.

[24] WANG Zhi-liang, ZHANG Xue-qin, GU Ju-ming, YANG Hai-tao, NIE Jun, MA Gui-ping. Electrodeposition of alginate/chitosan layer-by-layer composite coatings on titanium substrates [J]. Carbohydrate Polymers, 2014, 103: 38−45.

[25] RINAUDO M, PAVLOV G, DESBRIÈRES J. Influence of acetic acid concentration on the solubilization of chitosan [J]. Polymer, 1999, 40: 7029−7032

[26] JANES K A, CALVO P, ALONSO M J. Polysaccharide colloidal particles as delivery systems for macromolecules [J]. Advanced Drug Delivery Reviews, 2001, 47: 83−97.

[27] ANTUNES J C, PEREIRA C L, MOLINOS M, FERREIRA-DA-SILVA F, DESSÌ M, GLORIA A, AMBROSIO L, GONCALVES R M, BARBOSA M A. Layer-by-layer self-assembly of chitosan and poly(γ-glutamic acid) into polyelectrolyte complexes [J]. Biomacromolecules, 2011, 12: 4183−4195.

[28] FANG Jian-jun, ZHANG Yun, YAN Shi-feng, LIU Zhi-wen, HE Shi-ming, CUI Lei, YIN Jing-bo. Poly(L-glutamic acid)/chitosan polyelectrolyte complex porous microspheres as cell microcarriers for cartilage regeneration [J]. Acta Biomaterialia, 2014, 10: 276−288.

[29] JAMESH M I, WU G S, ZHAO Y, MCKENZIE D R, BILEK M M M, CHU P K. Electrochemical corrosion behavior of biodegradable Mg−Y−RE and Mg−Zn−Zr alloys in Ringer's solution and simulated body fluid [J]. Corrosion Science, 2015, 91: 160−184.

[30] LIM T S, RYU H S, HONG S H. Electrochemical corrosion properties of CeO_2-containing coatings on AZ31 magnesium alloys prepared by plasma electrolytic oxidation [J]. Corrosion Science, 2012, 62: 104−111.

[31] ANDREEVA D V, FIX D, MÖHWALD H, SHCHUKIN D G. Buffering polyelectrolyte multilayers for active corrosion protection [J]. Journal of Materials Chemistry, 2008, 18: 1738−1740.

[32] CARNEIRO J, TEDIM J, FERREIRA M G S. Chitosan as a smart coating for corrosion protection of aluminum alloy 2024: A review [J]. Progress in Organic Coatings, 2015, 89: 348−356.

[33] FU Jin-hong, JI Jian, YUAN Wei-yong, SHEN Jia-cong. Construction of anti-adhesive and antibacterial multilayer films via layer-by-layer assembly of heparin and chitosan [J]. Biomaterials, 2005, 26: 6684−6692.

[34] ZHAN Jie-zhao, WANG Lin, LIU Sa, CHEN Jun-jian, REN Li, WANG Ying-jun. Antimicrobial hyaluronic acid/poly(amidoamine) dendrimer multilayer on poly(3-hydroxybutyrate-co-4-hydroxybutyrate) prepared by a layer-by-layer self-assembly method [J]. ACS Applied Materials & Interfaces 2015, 7: 13876−13881.

[35] ZHUK I, JARIWALA F, ATTYGALLE A B, WU Y, LIBERA M R, SUKHISHVILI S A. Self-defensive layer-by-layer films with bacteria-triggered antibiotic release [J]. ACS Nano, 2014, 8: 7733−7745.

镁合金 AZ31 表面层层组装壳聚糖/聚谷氨酸涂层的体外耐蚀与抗菌性能

崔蓝月[1,2]，徐 霁[1]，陆 娜[1]，曾荣昌[1,2]，邹玉红[3]，李硕琦[1,2]，张 芬[1,2]

1. 山东科技大学 材料科学与工程学院，青岛 266590；
2. 山东科技大学 矿山灾害预防与控制国家重点实验室，青岛 266590；
3. 山东科技大学 化学与环境工程学院，青岛 266590

摘 要：镁合金表面功能化需要获得具有良好耐蚀性和抗菌性的表面。基于壳聚糖与聚谷氨酸之间的静电吸附作用，利用层层组装方法在镁合金 AZ31 表面获得一种既耐蚀又抗菌的涂层。利用高分辨扫描电子显微镜、傅里叶红外光谱仪以及电化学测试对这种功能涂层进行了表面形貌、化学成分以及耐蚀性能表征。通过平板计数法评定该涂层耐金黄葡萄球菌的性能。结果表明，该涂层具有良好的耐蚀性与抗菌性。

关键词：镁合金；腐蚀；层层组装；壳聚糖；抗菌性能

(Edited by Sai-qian YUAN)